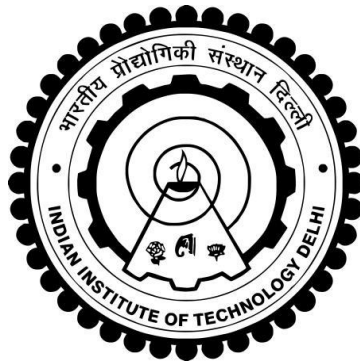


**PERFORMANCE ANALYSIS AND CONTROL OF A
REDUCED SWITCH MULTILEVEL INVERTER FED
PERMANENT MAGNET SYNCHRONOUS MOTOR
DRIVE**

POONAM JAYAL



**DEPARTMENT OF ELECTRICAL ENGINEERING
INDIAN INSTITUTE OF TECHNOLOGY DELHI
DECEMBER 2020**

© Indian Institute of Technology Delhi (IITD), New Delhi, 2020

**PERFORMANCE ANALYSIS AND CONTROL OF A
REDUCED SWITCH MULTILEVEL INVERTER FED
PERMANENT MAGNET SYNCHRONOUS MOTOR
DRIVE**

by

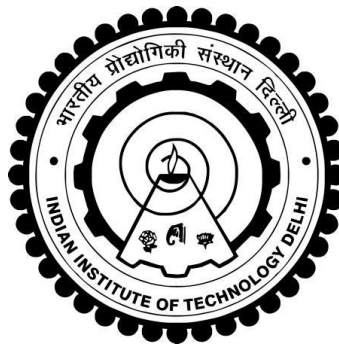
POONAM JAYAL

Department of Electrical Engineering

Submitted

in fulfillment of the requirements of the degree of DOCTOR OF PHILOSOPHY

to the



INDIAN INSTITUTE OF TECHNOLOGY DELHI

DECEMBER 2020

CERTIFICATE

This is to certify that the dissertation titled “**Performance Analysis and Control of a Reduced Switch Multilevel Inverter Fed Permanent Magnet Synchronous Motor Drive**”, being submitted by **Ms. Poonam Jayal** to the Department of Electrical Engineering, Indian Institute of Technology Delhi, for the award of the degree of Doctor of Philosophy, is a record of the bonafide research work carried out by her under my guidance and supervision.

Ms. Poonam Jayal has fulfilled the requirements for the submission of this thesis, which to my knowledge has reached the requisite standard. The results obtained herein have not been submitted in part or in full to any other University or Institute for the award of any degree.

Professor G. Bhuvaneswari
Department of Electrical Engineering
Indian Institute of Technology Delhi
New Delhi-110016, India

Date: 15.09.2020

ACKNOWLEDGEMENTS

At the outset, I would like to express my heartfelt thanks to the almighty for blessing me with this much awaited day when I have finally got the opportunity to pen down my feelings of gratitude and accomplishment to mark the culmination of this wonderful five year long journey.

My foremost and deepest gratitude to **Prof. G. Bhuvaneswari** for not only being my PhD supervisor, but also my mentor and a great pillar of strength. Working under her supervision has been a privilege and honour. Her resourceful inputs, excellent foresight, willingness to pay heed to my ideas and complementing them with her thoughtful suggestions, have been immensely useful during my course of research. I am grateful and deeply indebted to her for constantly motivating and imbibing in me the true research acumen. I have been genuinely blessed to have her in a pivotal role in this ‘wonderful’ journey.

I would also like to sincerely thank all the SRC members **Dr. Ramkrishan Maheshwari, Dr. Anandarup Das, and Dr. Ashu Verma** for providing me their valuable insights, suggestions and encouragement throughout my research work.

My heartfelt thanks to late **Prof. K R. Rajagopal**, my former supervisor, for identifying my research potential and entrusting me with this great responsibility. It was truly unfortunate to lose him in the early years of my research. He will always be missed!

I am thankful to IIT Delhi for providing the research facilities and **Visveswaraya PhD Scheme** supported by Department of Electronics and Information Technology (**DEITY**) for providing my research fellowship.

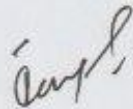
. Thanks are due to **Sh. Srichand, Sh. Puran Singh, Sh. Jitendra Kumar** and **Sh. Jagbir Singh** of PG Machines Lab and Departmental Workshop and **Sh. Dhan Raj Singh** and late **Sh. Suresh Chand** of UG Machines Lab, IIT Delhi, for their sustained help and for providing me the facilities to carry out my experimental work.

My journey at IIT Delhi would have been incomplete without the wonderful camaraderie that I shared with some of my research scholar and M.Tech friends. I would like to extend special thanks to my fellow research scholars **Mr. Sreejith Ravindran, Ms. Nibedita Parida, Mr. Deepu Vijay M, Mr. Pradyumna Ranjan Ghosh, Ms. Swagata Mapa, Ms. Samiksha Rawat, Mr. Saurabh Shukla, Mr. Rupam Basak and Mr. Tassaduq Hussain** for their indispensable technical as well as moral support. I would also like to thank my friends, **Mr. Sourabh Khandelwal, Ms. Kartika Haridas, Mr. Harsha Vardhan, Mr. Narsimhulu, Mr. Vishal, Mr. Ebin Mathew, Ms Neha Beniwal, Ms. Chestha Jain, Mr. Sritam Jena, Ms. Nidhi Bisht, Mr. Rajat , Mr. Rahul Sharma, Mr. Sukrashis, Ms. Nidhi Mishra, Dr. Shadab Murshid and Dr. Saurabh Shukla** for their tremendous love and support.

This long journey would have been impossible without the love and support of my family members. My foremost and deepest thanks to my father late **Sh. Dinesh Chandra Nautiyal** and my mother **Ms. Bhawani Nautiyal** for their unconditional love and blessings and for inspiring me to pursue my passions in life. I owe special thanks to my beloved husband, **Mr. Vipul Jayal**, for having faith in my capabilities and for always inspiring me to think big and do better. These five years of our long-distance relationship, owing to my PhD, will truly remain as a memorable experience of our lives. A huge

appreciation to my lovely kids **Vihaan** and **Nandini** for always being my bundles of joy, giving me that inner sense of complacency, which has always been a morale booster. My heartfelt thanks to my father-in-law **Sh. Harish Chandra Jayal**, my mother-in-law **Ms. Shanti Jayal** and my brother-in-law **Mr. Vaibhav Jayal** for being with me through thick and thin and providing me their constant love and moral support. Last but not the least, special thanks to my beautiful and loving sisters **Ms. Kanchan Chamola** and **Dr. Bhavana Nautiyal** for being there for me always!

I pray the Almighty for His benediction in my future endeavors too.



(Poonam Jayal)

New Delhi:15.09.2020

2015EEZ8301

ABSTRACT

Adjustable speed drives (ASDs) have emerged as the work horses of industries with a perspective of making the industrial processes more efficient and controllable. Permanent magnet synchronous motor (PMSM) drives are gradually emerging as the first choice of the ASD markets competing with variable speed induction motor and DC motor drives, due to their multifarious advantages like compact rotor structure, high power density, absence of rotor losses, better efficiency and excellent controllability. The advent of high-power semiconductor devices and power converter circuits controlled by high speed microprocessors have enabled PMSM drives to come a long way for low power servo applications ranging from 0.1kW to 10kW, and for high power applications up to 250kW.

Field oriented control (FOC) and direct torque control (DTC) are two important control techniques adopted for achieving speed and torque control in AC motor drives, mostly driven by a 2-level voltage source inverter. However, at higher power levels multi-level inverters (MLI) are employed to feed the motor drive in order to reduce the (dv/dt) stress across the power devices and to obtain a reasonably good response even with lower switching frequencies. Renowned MLI topologies such as neutral point clamped inverter (NPC), cascaded H bridge inverter (CHB) and flying capacitor inverter use too many devices and active and passive elements. In this context reduced switch MLIs prove to be meritorious over the conventional MLI topologies in terms of being cost-effective and more reliable (due to the reduced number of elements). Several modulation schemes exist for controlling the magnitude and harmonic content of the output voltage in any MLI; space vector pulse width modulation (SVPWM) being the most desirable with its property

of imparting better DC bus utilization and lesser harmonic content in the output even at a lower switching frequency.

A reduced switch 5-level inverter, namely, the transistor clamped H bridge (TCHB) inverter, has been explored in this work to feed a field-oriented controlled (vector-controlled) PMSM of 3.5 kW rating. As a prelude to this, a 2-level inverter controlled by SVPWM technique is implemented in Simulink/ MATLAB environment, to power a vector-controlled PMSM drive. The performance of the drive under different operating conditions such as starting, steady state operation at different speeds and torques, load perturbation, torque perturbation and speed reversal has been investigated in simulation and validated using a laboratory prototype of the 2-level inverter fed FOC PMSM drive. A simplified methodology, using a DSP and the Embedded coder toolbox from Mathworks, is adopted for the sensor based vector control of a surface mounted PMSM (SPMSM) drive for low values of speeds where saliency based sensorless tracking methods cannot be employed easily. Embedded coder generates the processor specific code in the MATLAB/Simulink platform itself, obviating the need for elaborate DSP programming. It enables easier rotor position and speed measurement using the enhanced quadrature encoder pulse (eQEP) module of the DSP.

A novel reduced switching analysis based SVPWM algorithm has been proposed for any (2^n+1) -level inverter ($n=1,2,3$ etc. yielding 3,5,9... level inverters) which allows a step wise translation of the space vector diagram (SVD) of the (2^n+1) -level inverter to a basic 2-level by using pivot vectors at 'n' different levels. The proposed SVPWM algorithm also elucidates and establishes that the switching combinations of the entire

(2^n+1) -level SVD, with 6^n small hexagons can be derived by investigating the switching combinations of merely a set of 2^n small (2-level) hexagons, thereby reducing the memory requirements for lookup tables and computation time of the processor. The successful implementation of this novel SVPWM algorithm has been demonstrated for 3-level and 5-level NPC and CHB inverter topologies.

This novel SVPWM algorithm is proposed as an improved modulation scheme for the TCHB 5-level inverter feeding a vector-controlled PMSM drive. In addition to simulation results, experimental results obtained from a laboratory prototype of the three phase TCHB inverter, running the SVPWM code using a DSP and Embedded Coder, infer that the drive offers excellent dynamic response, along with a very good steady state response with precise speed and torque outputs.

The TCHB inverter fed PMSM drive is also explored as one of the important powertrain components for electric vehicle (EV) applications. To demonstrate the viability of this inverter- motor duo for EV applications, wide speed operation of the MLI-fed PMSM drive is investigated using the field-weakening control. The response of the drive demonstrates that the proposed SVPWM algorithm helps the TCHB inverter to control the drive effectively and accurately over a wide range of speeds which would allow this drive unit to be used in a light motor vehicle. Further, to exhibit the efficient operation of the TCHB inverter for EV applications, a loss analysis of the TCHB inverter is presented using a simplified model for switching and conduction losses. This MATLAB/Simulink based simplified methodology is also proposed as a generalized methodology for developing the loss model for any MLI topology. From the loss

calculations carried out using this model, it is evident that the TCHB losses are much lower than a 5-level CHB inverter.

Finally, direct torque control (DTC) also has been implemented with a 5-level TCHB inverter fed PMSM drive. Further, an objective comparison of DTC and FOC has been carried out to bring out their relative advantages and disadvantages. In all, this work is an effort to investigate the use of a reduced switch 5-level inverter fed PMSM drive for a light weight EV application where accurate speed control has been achieved for a wide range of speed. Also, to utilize the DC bus effectively, a novel SVPWM algorithm has been proposed, designed, modeled, simulated and implemented in hardware.

सारांश

एडजस्टेबल स्पीड ड्राइव (ए एस डी) औद्योगिक प्रक्रियाओं को अधिक कुशल और नियंत्रणीय बनाने के परिप्रेक्ष्य के साथ उभर रहे हैं। परमानेंट मैग्नेट सिन्क्रोनस मोटर (पी एम एस एम) ड्राइव धीरे-धीरे ए एस डी बाजारों की पहली पसंद के रूप में उभर रहे हैं, जो कॉम्पैक्ट रोटर संरचना, उच्च शक्ति घनत्व, रोटर हानियों की अनुपस्थिति, बेहतर दक्षता और उत्कृष्ट नियंत्रणीयता जैसे विविध लाभों के कारण परिवर्तनीय गति वाले इंडक्शन मोटर और डीसी मोटर ड्राइव के साथ प्रतिस्पर्धा कर रहे हैं। उच्च गति माइक्रोप्रोसेसर द्वारा नियंत्रित उच्च शक्ति सेमीकंडक्टर उपकरणों और पावर कन्वर्ट सर्किट के आगमन ने पीएमएसएम ड्राइव को 0.1 किलोवाट से 10 किलोवाट तक कम पावर सर्वो अनुप्रयोगों के लिए एक लंबा रास्ता तय करने और 250 किलोवाट तक उच्च शक्ति अनुप्रयोगों के लिए सक्षम किया है।

फील्ड ओरिएंटेड कंट्रोल और डाइरेक्ट टार्ग कंट्रोल ए सी मोटर ड्राइव में गति और टॉर्क कंट्रोल प्राप्त करने के लिए अपनाई जाने वाली दो महत्वपूर्ण नियंत्रण तकनीकें हैं, जो ज्यादातर 2-स्तरीय वोल्टेज स्रोत इन्वर्टर द्वारा संचालित होती हैं। हालांकि, उच्च शक्ति स्तर पर बिजली उपकरणों में (डीवी/डीटी) तनाव को कम करने और कम स्विचन आवृत्तियों के साथ भी यथोचित प्रतिक्रिया प्राप्त करने के लिये बहु स्तरीय इन्वर्टर द्वारा चालित मोटर ड्राइव का प्रयोग किया जाता है। न्यूट्रल प्वाइंट क्लैप्ड इन्वर्टर (एन पी सी), कैस्केडड एच ब्रिज इन्वर्टर (सी एच बी) और फ्लाइंग कैपेसिटर इन्वर्टर जैसे प्रसिद्ध एमएलआई टोपोलोजी बहुत सारे उपकरणों और एक्टिव और पैसिव तत्वों का उपयोग करते हैं। इस संदर्भ में कम स्विच वाले एम एल आई लागत प्रभावी और अधिक विश्वसनीय होने के कारण पारंपरिक एम एल आई टोपोलोजियों से ज्यादा सराहनीय साबित होते हैं (तत्वों की कम संख्या के कारण)। किसी भी एम एल आई में आउटपुट वोल्टेज के परिमाण और हार्मोनिक सामग्री को नियंत्रित करने के लिए कई मॉड्यूलेशन योजनाएं मौजूद हैं; स्पेस वेक्टर पल्स विड्थ मॉड्यूलेशन (एसवीपीडब्ल्यूएम) बेहतर डीसी बस उपयोग प्रदान करने और कम स्विचिंग आवृत्ति पर भी कम हार्मोनिक सामग्री प्रदान करने के अपने गुण के कारण सबसे वांछनीय है।

इस कार्य में 3.5 किलोवाट रेटिंग के फील्ड ओरिएंटेड कंट्रोल (वेक्टर-कंट्रोल) पीएमएसएम को फीड करने के लिए - ट्रांजिस्टर क्लैंप एच ब्रिज (टीसीएचबी) इन्वर्टर नामक एक कम स्विच वाले 5-लेवल इन्वर्टर का विस्तारपूर्वक विश्लेषण किया गया है। इसकी प्रस्तावना के रूप में पहले एसवीपीडब्ल्यूएम तकनीक द्वारा नियंत्रित 2-स्तरीय इन्वर्टर को सिमुलिक/मैटलैब वातावरण में लागू किया गया है। विभिन्न ऑपरेटिंग परिस्थितियों में ड्राइव के प्रदर्शन जैसे विभिन्न गति और टॉर्क, लोड क्षोभ, टॉर्क क्षोभ और गति उत्क्रमण की सिमुलेशन में जांच की गई है और 2-स्तरीय इन्वर्टर फेड फील्ड ओरिएंटेड कंट्रोल पीएमएसएम ड्राइव के प्रयोगशाला प्रोटोटाइप का उपयोग करके मान्य किया गया है। एक सरलीकृत पद्धति, एक डीएसपी और मैथवर्क्स से एम्बेडेड कोडर टूलबॉक्स को सरफेस माउंटेड पीएमएसएम (एसपीएमएसएम) ड्राइव के सेंसर आधारित वेक्टर नियंत्रण के लिए अपनाया गया है जहां सेलियन्सी पर आधारित सेंसरलेस ट्रैकिंग विधियों को आसानी से नियोजित नहीं किया जा सकता है। एम्बेडेड कोडर मैटलैब/सिमुलिक प्लेटफॉर्म में ही प्रोसेसर विशिष्ट कोड उत्पन्न करता है, जो विस्तृत डीएसपी प्रोग्रामिंग की आवश्यकता को समाप्त करता है। यह डीएसपी के एनहांसड क्वाडरेचर एन्कोडर पल्स (ई क्यू ई पी) मॉड्यूल का उपयोग करके आसान रोटार स्थिति और गति माप को सक्षम बनाता है।

इस कार्य में एक कम स्विचिंग विश्लेषण पर आधारित नए एसवीपीडब्ल्यूएम एल्गोरिदम का प्रस्ताव किया गया है जो 'n' विभिन्न स्तरों पर धुरी वेक्टर का उपयोग करके किसी भी (2^n+1) स्तर के इन्वर्टर ($n=1,2,3$ आदि जैसे 3,5,9 स्तर) को एक बुनियादी 2-स्तर के इन्वर्टर में अनुवाद करने की अनुमति देता है। प्रस्तावित एसवीपीडब्ल्यूएम एल्गोरिदम यह भी स्पष्ट और स्थापित करता है कि $6n$ छोटे हेक्सागनों के साथ पूरे (2^n+1) - स्तर के स्पेस वेक्टर डायग्राम (एसवीडी) के स्विचिंग संयोजनों को केवल 2^n छोटे (2-स्तर) हेक्सागनों के स्विचिंग संयोजनों की जांच करके प्राप्त किया जा सकता है, जिससे प्रोसेसर के लुकअप टेबल और गणना समय के लिए कंप्यूटर की मैमोरी आवश्यकताओं को कम किया जा सकता है। इस नए

एसवीपीडब्ल्यूएम एल्गोरिदम के सफल कार्यान्वयन को 3-स्तरीय और 5-स्तरीय एनपीसी और सीएचबी इन्वर्टर टोपोलोजी के लिए प्रदर्शित किया गया है।

इस नए एसवीपीडब्ल्यूएम एल्गोरिदम को 5-स्तरीय टीसीएचबी इन्वर्टर के लिए एक बेहतर मॉड्यूलेशन योजना के रूप में प्रस्तावित किया गया है। सिमुलेशन परिणामों के अलावा, एक डीएसपी और एम्बेडेड कोडर का उपयोग करके एसवीपीडब्ल्यूएम कोड चलाते हुए एक थ्री फेज टीसीएचबी इन्वर्टर के प्रयोगशाला प्रोटोटाइप से प्राप्त प्रयोगात्मक परिणाम सटीक ड्राइव प्रदर्शन, जैसे गति और टार्क आउटपुट, प्रदान करते हैं।

टीसीएचबी इन्वर्टर फेड पीएमएसएम ड्राइव को इलेक्ट्रिक वाहन (ईवी) अनुप्रयोगों के लिए महत्वपूर्ण पावरट्रेन घटकों में से एक के रूप में भी खोजा गया है। ईवी अनुप्रयोगों के लिए इस इन्वर्टर-मोटर जोड़ी की व्यवहार्यता प्रदर्शित करने के लिए, एमएलआई-फेड पीएमएसएम ड्राइव के व्यापक गति संचालन की जांच फील्ड वीकनिंग नियंत्रण से भी की गई है। ड्राइव की प्रतिक्रिया दर्शाता है कि प्रस्तावित एसवीपीडब्ल्यूएम एल्गोरिदम टीसीएचबी इन्वर्टर ड्राइव को प्रभावी ढंग से और सटीक रूप से गति की एक विस्तृत श्रृंखला पर नियंत्रित करने में मदद करता है जो इस ड्राइव इकाई को हल्के मोटर वाहन में उपयोग करने की अनुमति देगा। इसके अलावा, ईवी अनुप्रयोगों के लिए टीसीएचबी इन्वर्टर के कुशल संचालन को प्रदर्शित करने के लिए, टीसीएचबी इन्वर्टर का लॉस विश्लेषण स्विचिंग और कंडक्शन हानियों के लिए एक सरलीकृत मॉडल का उपयोग करके प्रस्तुत किया गया है। यह मैटलैब/सिमुलिक आधारित सरलीकृत पद्धति भी किसी भी एमएलआई टोपोलॉजी के लिए लॉस मॉडल विकसित करने के लिए एक सामान्यीकृत पद्धति के रूप में प्रस्तावित है। इस मॉडल का उपयोग कर लॉस विश्लेषण से यह स्पष्ट है कि टीसीएचबी इन्वर्टर का नुकसान 5-स्तर के सीएचबी इन्वर्टर की तुलना में बहुत कम है।

अंत में, 5-स्तरीय टीसीएचबी इन्वर्टर फेड पीएमएसएम ड्राइव के साथ डायरेक्ट टॉर्क कंट्रोल (डीटीसी) को भी लागू किया गया है। इसके अलावा, डीटीसी और एफओसी की वस्तुनिष्ठ तुलना उनके

सापेक्ष लाभ और नुकसान को सामने लाने के लिए की गई है । कुल मिलाकर, इस कार्य में हल्के वजन वाले ईवी एप्लिकेशन के लिए कम स्विच वाले 5-स्तरीय इन्वर्टर फेड पीएमएसएम ड्राइव के उपयोग की जांच करने का प्रयास है जहां एक विस्तृत रेंज के लिए सटीक गति नियंत्रण हासिल की गई है । इसके अलावा, डीसी बस का प्रभावी ढंग से उपयोग करने के लिए नए एसवीपीडब्ल्यूएम एल्गोरिदम को डिजाइन, मॉडल और सिमुलेट करने के साथ ही हार्डवेयर में भी लागू किया गया है।

TABLE OF CONTENTS

Certificate	i	
Acknowledgements	iii	
Abstract	vii	
Table of Contents	xv	
List of Figures	xix	
List of Tables	xxvii	
List of Abbreviations	xxix	
List of Symbols	xxxii	
CHAPTER I	INTRODUCTION	1-14
1.1	General	1
1.2	State of the Art	4
1.3	Scope of Work	7
1.4	Organization of the Thesis	11
CHAPTER II	LITERATURE REVIEW	15-27
2.1	General	15
2.2	Control Techniques for PMSM Drives	15
2.2.1	Vector Controlled PMSM Drives	16
2.2.2	Direct Torque Control Based PMSM Drives	17
2.2.3	Field-Weakening Control Based PMSM Drives	18
2.3	Multilevel Inverters	19
2.3.1	Multilevel Inverter Topologies	20
2.3.2	Modulation Schemes for Multilevel Inverters	21
2.3.3	Loss Calculations for Multilevel Inverters	23
2.4	PMSM Drives for Electric Vehicle Applications	24
2.5	Transistor-Clamped H Bridge Reduced Switch MLI Topology	25
2.6	Research Gaps	26
2.7	Conclusion	27
CHAPTER III	MODELING, SIMULATION AND HARDWARE IMPLEMENTATION OF A 2-LEVEL VSI FED VECTOR CONTROLLED PMSM DRIVE	29-66
3.1	General	29
3.2	Mathematical Model of a Surface Mounted PMSM	30
3.3	Vector Control of a PMSM Drive	33
3.3.1	Principle of Vector Control for a PMSM	33
3.3.2	Vector Control of a 2-Level VSI Fed PMSM Drive	35
3.4	Simplified Encoder-Based Vector Control of PMSM Drive	37
3.4.1	Working Principle of an Encoder	37
3.4.2	Configuration and Utilization of the Enhanced Quadrature Encoder Pulse (eQEP) Module of a DSP on the Embedded Coder	39

3.4.2.1	Rotor Position Detection Using eQEP Module of the DSP	41
3.4.2.2	Speed Detection Using eQEP Module of the DSP	42
3.5	Modulation Schemes for a 2-Level VSI	44
3.5.1	Sinusoidal Pulse Width Modulation Scheme for a 2-Level VSI	44
3.5.2	Space Vector Pulse Width Modulation Scheme for a 2-Level VSI	45
3.6	MATLAB-Based Modeling and Simulation of the 2-Level VSI Fed SPMSM Drive	51
3.7	System Configuration for Hardware Implementation of Vector Control of a SPMSM Triggered Using a 2-level VSI	54
3.8	Simulation Results and Discussion	57
3.9	Experimental Results and Discussion	60
3.10	Conclusion	66
CHAPTER IV REDUCED SWITCHING ANALYSIS - BASED NOVEL SVPWM FOR MULTILEVEL INVERTERS		67-104
4.1	General	67
4.2	Proposed Space Vector Algorithm	68
4.2.1	Proposed Space Vector Model	68
4.2.2	Detailed Implementation of the Proposed SVPWM Algorithm for Multilevel Inverters	70
4.2.2.1	Translation of the Reference Vector Down to a 2-Level SVD	71
4.2.2.2	Simplification of Switching Analysis Using the Proposed SVPWM Algorithm	71
4.2.3	A Simple Analogy behind the Concept of Reduced Switching Analysis in the Proposed SVPWM Algorithm	81
4.3	MATLAB/Simulink - Based Implementation of the Proposed SVPWM Algorithm for MLI Topologies	83
4.4	System Configuration for Hardware Implementation of the Proposed SVPWM Algorithm for MLI Topologies	85
4.5	Simulation Results and Discussion	87
4.5.1	Steady State Response for Different MLI Topologies Using the Proposed SVPWM Scheme	89
4.5.2	Dynamic Response for MLI Topologies Triggered with the Proposed SVPWM Scheme	93
4.5.3	Comparison of SVPWM Scheme with Carrier-Based Modulation Scheme	95
4.6	Experimental Results and Discussion	98
4.7	Comparative Analysis of the Proposed SVPWM Algorithm with the Existing SVPWM Algorithms	102
4.8	Conclusion	104
CHAPTER V ENHANCED MODULATION SCHEME TRRIGERED REDUCED SWITCH 5-LEVEL INVERTER		105-132
5.1	General	105

5.2	Transistor-Clamped H Bridge Reduced Switch 5-Level Inverter	106
5.2.1	Topology	106
5.2.2	Conventional Modulation Schemes for the TCHB Inverter	109
5.2.3	Comparison with other MLI Topologies	112
5.3	Proposed Modulation Scheme for the TCHB Inverter	113
5.4	MATLAB-Based Modeling and Simulation of the TCHB Inverter	115
5.5	System Configuration for Hardware Implementation of the Proposed SVPWM Algorithm for the TCHB Inverter	119
5.6	Simulation and Experimental Results and Discussions	120
5.6.1	Steady State Response of TCHB Inverter Feeding an RL Load Triggered with Conventional and Proposed Modulation Schemes	120
5.6.2	Dynamic Response of TCHB Inverter Feeding an RL Load Triggered with Conventional and Proposed Modulation Schemes	126
5.7	Control of Neutral Point Voltage Deviation in the TCHB Inverter While Using the Proposed SVPWM Scheme	129
5.8	Conclusion	131
CHAPTER VI TRANSISTOR-CLAMPED H BRIDGE INVERTER DRIVEN PERMANENT MAGNET SYNCHRONOUS MOTOR DRIVE FOR EV APPLICATIONS		133-170
6.1	General	133
6.2	Vector Control of the TCHB Inverter Driven PMSM for Electric Vehicle Applications	135
6.3	Simplified Loss Analysis Model for the TCHB Inverter	137
6.3.1	Conduction Loss Model for the 5-Level TCHB Inverter	138
6.3.2	Switching Loss Model for the 5-Level TCHB inverter	143
6.4	Validation of the TCHB Inverter Loss Model	145
6.4.1	Validation of Switching Losses for the TCHB Inverter	146
6.4.2	Validation of Conduction Losses for the TCHB Inverter	150
6.5	Loss Model for a 5-Level CHB Inverter	152
6.6	MATLAB-Based Modeling and Simulation Results of the Proposed SVPWM Triggered TCHB Inverter Fed PMSM Drive	158
6.6.1	Steady State and Dynamic Response of the PMSM Drive	158
6.6.2	Loss Analysis-Based Evaluation of the TCHB Inverter Fed Vector Controlled PMSM Drive Triggered by the Modified SVPWM Scheme	160
6.7	System Configuration and Experimental Results for Hardware Implementation of the Proposed SVPWM Triggered TCHB Inverter Fed PMSM Drive	162
6.7.1	Steady State Performance of PMSM Drive at Constant Load and at a Constant Speed of 1000 rpm	165
6.7.2	Dynamic Performance of the TCHB Inverter Fed Vector Controlled PMSM Drive	167
6.8	Conclusion	169

CHAPTER VII	MODELING, SIMULATION AND ANALYSIS OF FIELD-WEAKENING CONTROL FOR THE 5-LEVEL TCHB INVERTER FED VECTOR-CONTROLLED PMSM DRIVE	171-192
7.1	General	171
7.2	Modes of PMSM Operation: A Summary	172
7.3	Principle of Field Weakening Control for a Surface Mounted PMSM	176
7.4	System Configuration for the Operation of the Five Level TCHB Inverter Fed PMSM Drive Over a Wide Speed Range	178
7.5	Limitation on Maximum Attainable Speed by a PMSM in the Field- Weakening Zone	181
7.6	MATLAB Based Modeling for a 5-Level TCHB Inverter Fed PMSM Drive Over a Wide Speed Range	184
7.7	Simulation Results and Discussion	189
7.8	Conclusion	192
CHAPTER VIII	MODELING, SIMULATION AND ANALYSIS OF DIRECT TORQUE CONTROL FOR THE 5-LEVEL TCHB INVERTER FED PMSM DRIVE	193-212
8.1	General	193
8.2	System Configuration for Implementation of DTC for a VSI Fed PMSM Drive	194
8.3	MATLAB Based Modeling for DTC of VSI Fed PMSM Drive	197
8.4	Simulation Results and Discussions	201
8.5	Comparative Performance Analysis of Vector-Controlled and Direct Torque Controlled VSI Fed PMSM Drives	207
8.6	Conclusion	210
CHAPTER IX	MAIN CONCLUSIONS AND SUGGESTIONS FOR FUTURE WORK	211-219
9.1	General	211
9.2	Main Conclusions	212
9.3	Suggestions for Future Work	216
REFERENCES		219-233
APPENDIX-A		235
APPENDIX-B		237
APPENDIX-C		239-256
LIST OF PUBLICATIONS		259
BIO-DATA		261

LIST OF FIGURES

- Fig. 3.1 Phasor Diagram of a PMSM
- Fig. 3.2 Phasor diagram of constant torque control strategy for vector control of a PMSM
- Fig. 3.3 Block schematic for vector control of a two-level voltage source inverter (VSI) fed PMSM drive
- Fig. 3.4 Encoder output pulses for (a) Clockwise rotation (b) Counterclockwise rotation (a)-(b)
- Fig. 3.5 Configuration of eQEP module (a) General block settings (b) Position counter block settings (c) Speed calculation block settings (a)-(b)
- Fig. 3.6 MATLAB/Simulink model for capturing rotor position using eQEP module of embedded coder toolbox.
- Fig. 3.7 MATLAB/Simulink model for determining rotor speed from the position obtained from eQEP module
- Fig. 3.8 MATLAB/Simulink model for capturing PMSM speed using eQEP module
- Fig. 3.9 2-Level voltage source inverter
- Fig. 3.10 Basic principle of SPWM for a 2-level VSI
- Fig. 3.11 2- level space vector diagram
- Fig. 3.12 MATLAB/Simulink model of a SPMSM
- Fig. 3.13 MATLAB/Simulink model of a 2-level VSI fed PMSM drive
- Fig. 3.14 MATLAB/Simulink model for implementing SPWM for a 2-Level VSI
- Fig. 3.15 MATLAB/Simulink model for implementing SVPWM for a 2-level VSI
- Fig. 3.16 MATLAB/Simulink model for current sensing using ADC on embedded coder platform
- Fig. 3.17 Experimental set-up for a 2-Level VSI fed PMSM drive
- Fig. 3.18 Experimental apparatus (a) Current Sensor Board (b) PMSM (a)-(b)
- Fig. 3.19 Encoder connections (a) Motor encoder terminals (b) Interfacing with QEP port A on the DSP board (a)-(b)
- Fig. 3.20 Connection diagram of PMSM encoder terminals with eQEP port of the DSP
- Fig. 3.21 Starting transients of the 2-level VSI fed vector controlled PMSM drive

- Fig. 3.22 Speed perturbation in a 2-level VSI fed vector controlled PMSM drive for a constant load
- Fig. 3.23 (a) Load perturbation in a 2-level VSI fed vector controlled PMSM drive for a constant speed (b) Zoomed view showing the speed retracting to its constant value at every load change
- Fig. 3.24 Speed reversal of a 2-level VSI fed vector controlled PMSM drive
- Fig. 3.25 Experimentally obtained encoder Pulses (a) A and B (counterclockwise) (a)-(b) (b) Index pulses
- Fig. 3.26 Experimental results for steady state response of 2-level VSI fed vector controlled PMSM drive at 1000 rpm (a) PWM generated voltage references for VSI (b) Rotor position from encoder (c) DAC outputs of reference and actual speeds with line voltage and line current (d) i_{sd}^* and i_{sd} actual (e) i_{sq}^* and i_{sq} actual.
- Fig. 3.27 Dynamic response of 2-level VSI fed vector controlled PMSM drive (a)-(b) (a) Speed tracking (b) Speed reversal
- Fig. 4.1 Five level SVD (a) Big Hexagons (1-6) (b) Small Hexagons (A1-F1) (a)-(b)
- Fig. 4.2 Pivot Vectors (a) Three-level (PV3) (b) Two-level (PV2) (c) Magnitude calculation of PV3 and PV2
- Fig. 4.3 Flowchart showing the translation of 5-level reference vector to 2-level
- Fig. 4.4 3-Level NPC inverter (a) Circuit configuration (b) 3-level SVD (a)-(b)
- Fig. 4.5 Reduced 2-level small hexagons of a 3-level SVD (a) A and D (a)-(c) (b) C and F (c) B and E
- Fig. 4.6 5-level Cascaded H Bridge inverter (a) Circuit configuration of a single phase (b) 5-level SVD
- Fig. 4.7 Sets of reduced 2-level hexagons yielding simplification in the switching analysis of a 5-level inverter (a) A1, D1, A4, D4 (b) C3, C6, F3, F6 (c) B2, B5, E2, E5
- Fig. 4.8 Flowchart showing implementation of Table 6.12 for simplification of phase 'a' switchings for a 5-level inverter
- Fig. 4.9 Simplifications in phase 'a' switchings
- Fig. 4.10 MATLAB/Simulink model for a 3-Level NPC inverter
- Fig. 4.11 MATLAB/Simulink model for a 5-Level NPC inverter (a) The complete model (b) Subsystem showing 5-Level to 3-Level translation

- (c) Subsystem showing 3-Level to 2-Level translation (d) Subsystem within the 2-level logic block of 4.11(a)
- Fig. 4.12 Experimental set-up for SVPWM triggered 3-level NPC inverter
- Fig. 4.13 Experimental set-up for SVPWM triggered 3-level CHB inverter
- Fig. 4.14 Firing pulse generation using a DSP and buffer board
- Fig. 4.15 Experimental set-up for SVPWM triggered 5-level CHB inverter
- Fig. 4.16 Firing pulses for phase 'a' of (a) 3-Level NPC inverter (b) 5-Level NPC inverter (c) 3-Level CHB inverter (d) 5-Level CHB inverter
- Fig. 4.17 Simulated voltage and current waveforms for the inverters (a)-(b) (a) 3-level CHB (b) 3-level NPC (a) 5-level CHB (b) 5-level NPC
- Fig. 4.18 Variation in voltage and current THD with change in switching frequency at a fixed MI and load
- Fig. 4.19 Variation in voltage and current THD with change in MI at a fixed switching frequency and load
- Fig. 4.20 Carrier-based PWM (IPD modulation) for a 3-Level NPC inverter
- Fig. 4.21 Carrier-based PWM (IPD modulation) for a 5-Level NPC inverter
- Fig. 4.22 Variation in THD (%) with change in modulation index at constant switching frequency and constant load (a)-(b) (a) Voltage THD (b) Current THD
- Fig. 4.23 Variation of fundamental line voltage (RMS) with change in MI for SVPWM and SPWM fed NPC inverters
- Fig. 4.24 Proposed SVPWM triggered inverter voltage and current waveforms for (a)-(b) (a) 3-level NPC (b) 3-level CHB (c) 5-level CHB and Harmonic spectrum of line voltages and currents for (d) 3-level NPC (e) 3-level CHB (f) 5-level CHB
- Fig. 4.25 Proposed SVPWM fed (a) 3-level CHB inverter line voltages (b) 5-level CHB inverter line currents
- Fig. 4.26 Response of the SVPWM triggered 3-level CHB inverter to variations in load
- Fig. 4.27 Response of the SVPWM triggered 3-level CHB inverter to variations in modulation index
- Fig. 5.1 Single-phase TCHB inverter with RL load
- Fig. 5.2 Operational modes of the single-phase TCHB inverter
- Fig. 5.3 Conventional level-shifted modulation schemes for the TCHB inverter with (a) Level-shifted carrier waves (b) Level-shifted modulating waves

- Fig. 5.4 Generation of firing pulses for single-phase TCHB inverter using conventional level-shifted modulation scheme of Figure 5.3(b)
- Fig. 5.5 Small hexagon A1 of a 5-level space vector diagram
- Fig. 5.6 Firing pulse generation using carrier based PWM for one phase of the TCHB inverter
- Fig. 5.7 Experimental set up of a three phase TCHB inverter feeding an RL load
- Fig. 5.8 Simulated and experimentally obtained gating pulses for three phase TCHB inverter feeding an RL load (a)&(b) Conventional Scheme (c) & (d) Proposed SVPWM Scheme
- Fig. 5.9 Simulation results for TCHB inverter feeding an RL load and triggered with the conventional carrier-based scheme (a) Line voltage and current (b) Harmonic spectrum of line voltage (c) Harmonic spectrum of current
- Fig. 5.10 Experimental results for TCHB inverter feeding an RL load and triggered with the conventional carrier-based scheme (a) Three phase line currents and single phase load voltage (b) Three phase line voltages (c) Harmonic spectrum of line voltage (d) Harmonic spectrum of line current
- Fig. 5.11 Simulation results for TCHB inverter feeding an RL load and triggered with the proposed modulation scheme (a) Line voltage and current (b) Harmonic spectrum of line voltage (c) Harmonic spectrum of current
- Fig. 5.12 Experimental results for TCHB inverter feeding an RL load and triggered with the proposed modulation scheme (a) Three phase line currents and single phase load voltage (b) Three phase line voltages (c) Harmonic spectrum of line voltage (d) Harmonic spectrum of line current
- Fig. 5.13 Variation of total harmonic distortion (THD) with modulation index for line voltage of TCHB inverter triggered with the conventional and proposed modulation schemes
- Fig. 5.14 Switching signals for (a) Carrier-based modulation scheme at 1700Hz (b) Proposed SVPWM based modulation scheme at 900 Hz
- Fig. 5.15 Redundant switching states of small hexagons (a) D1 (b) A4
- Fig. 5.16 Balanced capacitor voltages V_{C1} and V_{C2} for the proposed SVPWM fed TCHB inverter feeding an RL load as per parameters of Table 5.7
- Fig. 6.1 Block schematic of a battery-operated electric vehicle
- Fig. 6.2 TCHB fed PMSM drive configuration for an EV
- Fig. 6.3 Overall conduction loss model for the 5-level TCHB inverter
- Fig. 6.4 Per phase IGBT conduction loss model for the 5-level TCHB inverter

- Fig. 6.5 Per phase bridge diode conduction loss model for the TCHB inverter
- Fig. 6.6 Per phase feedback diode conduction loss model for the 5-level TCHB inverter
- Fig. 6.7 Expanded view of the logic blocks of Figure 6.6 for switching states (a)-(e) (a)P2 (b) P1
- Fig. 6.8 Energy versus current datasheet for IGBT SKM75GB12T4
- Fig. 6.9 Per phase switching loss model for TCHB inverter (a) Overall switching loss model (b) Expanded view for S_1 Loss of Figure 6.9(a)
- Fig. 6.10 Simulation image showing conduction and switching losses being displayed at 2kHz switching frequency and rated load of 7.3A for a single phase of the TCHB inverter
- Fig. 6.11 Gating pulses for one fundamental cycle of a TCHB inverter
- Fig. 6.12 Per phase IGBT conduction loss model for the 5-level CHB inverter
- Fig. 6.13 (a) Per phase feedback diode conduction loss model for the 5-level CHB inverter (b) Logic inside the subsystem of D_{1ON}
- Fig. 6.14 Logic blocks showing generation of D_{nON} labels from different states of 5-level CHB inverter (a) P2 (b) P1 (c) N1 (d) N2 (e) O
- Fig. 6.15 Vector controlled PMSM drive fed from a novel SVPWM based TCHB for an urban drive cycle (UDC) with the zoomed view for current and speed
- Fig. 6.16 Regenerative performance of the PMSM drive (a)Deceleration from 750 rpm to 250 rpm (b) Regenerated power in a PMSM drive based EV
- Fig. 6.17 Conduction and switching losses at 2kHz switching frequency and rated load of 7.3A for single phase CHB inverter
- Fig. 6.18 Variation of inverter losses (a) with variations in switching frequency at rated load (7.3A) (b) with changing load at a switching frequency of 2 kHz
- Fig. 6.19 PMSM and DC machine motor-generator set for experimentation
- Fig. 6.20 Experimental set-up of TCHB inverter fed PMSM drive
- Fig. 6.21 Steady state experimental results for vector control of the TCHB inverter fed PMSM drive triggered with the proposed SVM scheme at 1000 rpm and 15% of rated torque
- Fig. 6.22 Dynamic response of TCHB inverter fed PMSM drive showing (a) speed dynamics at a constant load (b) load perturbation at constant reference speed
- Fig. 6.23 Comparison of speed tracking for (a) 5-level TCHB inverter fed PMSM drive (b) 2-level inverter fed PMSM drive
- Fig. 7.1 The constant torque and constant power regions of operation of a PMSM

- Fig. 7.2 Voltage and current limit circles of (a) Surface mounted PMSM (b) Interior PMSM
- Fig. 7.3 Phasor Diagram of a SPMSM in the field-weakening zone
- Fig. 7.4 Block schematic of closed-loop operation of a PMSM over a wide speed range of operation
- Fig. 7.5 MATLAB/Simulink model of implementing wide speed range control for a SVPWM triggered 5-level TCHB or a 2-level VSI fed PMSM drive
- Fig. 7.6 MATLAB/Simulink Model of Various Subsystems of Figure 7.5 involved in the calculation of new values of i_{sd} and i_{sq} for Implementing Field Weakening Control in a PMSM Drive (a) Subsystem for calculating new value of i_{sd} (b) Zoomed subsystem (c) Subsystem for obtaining the new value of i_{sq} based on the new value of i_{sd} obtained in part (a)
- Fig. 7.7 MATLAB/Simulink Models of the following Subsystems of Figure 7.5 (a)-(c) (a) The FWC (b) Torque Angle Calculation Block (c) Airgap Flux Linkage Evaluation Block
- Fig. 7.8 Simulation results of SVPWM triggered 5L-TCHB inverter fed PMSM drive operation in the field-weakening zone (a) Characteristic waveforms of important parameters (b) Harmonic spectrum of the line currents and voltages
- Fig. 7.9 Simulation results of SVPWM triggered 2L-VSI fed PMSM drive operation in the field-weakening zone (a) Characteristic waveforms of important parameters (b) Harmonic spectrum of the line currents and voltages
- Fig. 7.10 Wide speed operation of SVPWM triggered 5l TCHB Inverter Fed PMSM Drive Ranging from 100 rpm to 4500 rpm
- Fig. 8.1 Block schematic for direct torque control of a two-level voltage source inverter (VSI) fed PMSM drive
- Fig. 8.2 Active switching vectors generated by a 2-Level VSI
- Fig. 8.3 Block schematic for SVPWM based DTC for a 2-level VSI fed PMSM drive
- Fig. 8.4 MATLAB/Simulink based DTC Model for a 2-level VSI fed PMSM drive
- Fig. 8.5 Expanded view of subsystems of Figure 8.4 for flux estimation
- Fig. 8.6 Expanded view of subsystems of Figure 8.4 for torque estimation (a)-(b) (a) Without using rotor position (b) Using rotor position
- Fig. 8.7 MATLAB/Simulink relay block for setting up the (a) 3-level torque hysteresis controller (b) 2-level flux hysteresis controller

- Fig. 8.8 Steady state response of a 2-level VSI fed DTC PMSM drive
- Fig. 8.9 Dynamic response of a 2-level VSI fed DTC PMSM drive with speed perturbations at constant load torque
- Fig. 8.10 Dynamic response of a 2-level VSI fed DTC PMSM Drive with load perturbations at constant speed
- Fig. 8.11 Steady state response of a 5-level TCHB fed DTC PMSM drive
- Fig. 8.12 Comparison of torque ripples for DTC-PMSM drive fed by (a) 2-level hysteresis controller based VSI (b) 5-level TCHB inverter
- Fig. 8.13 Comparison of torque pulsations for (a) 2-level VSI fed DTC PMSM drive using hysteresis comparators (b) 5-level TCHB inverter fed SVPWM based DTC PMSM drive using PI controllers (c) 5-level TCHB inverter fed FOC PMSM drive
- Fig. 8.14 (a) Zoomed torque pulsations for 8.13 (b) - (c); (b) Comparison of dynamic load torque response for 5-level TCHB inverter fed DTC PMSM drive and 5-level TCHB inverter fed FOC PMSM drive
- Fig. 8.12 Comparison of DTC and FOC PMSM Drive (a) Speed trajectory tracking (a)-(d) (b) Dynamic load torque tracking response (c) Zoomed view of torque pulsations (d) stator Current Response

LIST OF TABLES

Table 3.1	Variables Used in Modeling Equations
Table 3.2	Space Vectors for a 2-Level Voltage Source Inverter
Table 3.3	Seven-Segment Switching Sequence in One Sampling Interval
Table 4.1	Magnitude and Zone Allocation of PV3 and PV2
Table 4.2	Reference Vector Translational Levels
Table 4.3	Switching States for 3-level NPC Inverter (Phase ‘a’)
Table 4.4	Switching Sequence for Sector 1 of Small Hex A of 3-level NPC Inverter
Table 4.5	Switching States for Sector 1 of Small Hex A Based-on Table 4.4
Table 4.6	Relationship Established Between the Small Hexagons of a 3-Level SVD
Table 4.7	Switching States for 5-level CHB Inverter
Table 4.8	Switching Sequence for Sector 1 of Small Hex A1 of 5-level CHB Inverter (only 4 out of 7 segments shown)
Table 4.9	Switching States for Sector 1 of Small Hex A Based-on Table 4.8
Table 4.10	Relationship Established Between the Small and Big Hexagons of a 5-Level SVD
Table 4.11	Simplification in Switching Analysis Using the Proposed SVPWM
Table 4.12	Relationship Between Big and Small Hexagons of a 5-Level Inverter w.r.t Switching Sequence of Phase ‘a’ Devices
Table 4.13	Simulation Parameters Used for Different MLI Topologies
Table 4.14	Variation in Load at Fixed Modulation Index and Switching Frequency
Table 4.15	Variation in Modulation Index at Fixed Load and at Constant Switching Frequency
Table 4.16	Comparative Analysis of the Proposed Algorithm with the Existing Schemes
Table 5.1	Switching States for the TCHB Inverter
Table 5.2	Switching states of the TCHB inverter Showing Status of All Devices
Table 5.3	Comparison of TCHB Inverter with Conventional 5-level Inverters Based on Topological Structure
Table 5.4	Switching Sequence for Sector 1 - A1 of the TCHB Inverter
Table 5.5	Mapping of the Switching States with the TCHB Devices for Phase ‘a’
Table 5.6	Lookup Table for Phase ‘a’ Device Switchings of TCHB Inverter
Table 5.7	Simulation and Experimentation Parameters
Table 5.8	Simulation Results for Conventional Modulation Scheme Fed TCHB Inverter at Different Switching Frequencies

Table 5.9	Simulation Results for Proposed SVPWM Scheme Fed TCHB Inverter at Different Switching Frequencies
Table 5.10	Switching Alternatives for Sector 1 of Small Hexagon D1 for a 5-Level SVD
Table 6.1	IGBT and Power Diode Parameters
Table 6.2	Voltage Across IGBTs of the TCHB Inverter in ‘OFF’ State
Table 6.3	Simulation Parameters for Loss Model of the TCHB Inverter
Table 6.4	Simulation Results from TCHB Loss Model of Figure 6.10
Table 6.5	Switching Losses During ‘ON’ Transitions in a TCHB Inverter
Table 6.6	Switching Losses During ‘OFF’ Transitions in a TCHB Inverter
Table 6.7	Conduction Loss Calculations from TCHB Loss Model
Table 6.8	Switching States of the 5-level CHB Inverter
Table 6.9	Detailed Switching States of the 5-level CHB Inverter Showing Status of All Active and Passive Devices
Table 6.10	Specifications of an Experimental Prototype Developed for the Three-Phase TCHB Inverter Fed PMSM Drive
Table 8.1	Switching Table for a 2-Level VSI Fed DTC Drive

LIST OF ABBREVIATIONS

ASD	Adjustable Speed Drives
BLDC	Brushless DC Motor
CHB	Cascaded H Bridge
DAC	Digital to Analog Converter
dSPACE	Digital Signal Processing and Control Engineering
DSP	Digital Signal Processor
DTC	Direct Torque Control
eQEP	Enhanced Quadrature Encoder Pulse
ePWM	Enhanced Pulse Width Modulation
EMI	Electromagnetic Interference
EV	Electric Vehicle
FOC	Field-Oriented Control
FWC	Field-Weakening Controller
GPIO	General Purpose Input Output
IGBT	Insulated Gate Bipolar Transistor
IPD	In-phase Disposition
IPMSM	Interior Permanent Magnet Synchronous Motor
MATLAB	Matrix Laboratory
MI	Modulation Index
MLI	Multi-level Inverter
MTPA	Maximum Torque Per Ampere
MTPV	Maximum Torque Per Voltage
NEDC	New European Drive Cycle
NPC	Neutral Point-Clamped
NTV	Nearest Three Vector
PI	Proportional-Integral
PMSM	Permanent Magnet Synchronous Motor
PPR	Pulses Per Revolution

PV	Pivot Vector
PV3	Pivot Vector 3-Level
PV2	Pivot Vector 2-Level
PWM	Pulse Width Modulation
RMS	Root Mean Square
RPM	Revolutions per minute
SPMSM	Surface Mounted Permanent Magnet Synchronous Motor
SPWM	Sinusoidal Pulse Width Modulation
SVD	Space Vector Diagram
SV	Space Vector
SVPWM	Space Vector Pulse Width Modulation
TCHB	Transistor Clamped H Bridge
THD	Total Harmonic Distortion
UDC	Urban Driving Cycle
VSI	Voltage Source Inverter

LIST OF SYMBOLS

B	Viscous friction coefficient ($\text{kg}\cdot\text{m}^{-1}\cdot\text{s}^{-1}$)
E_b	Back EMF of motor (V)
E_{on}	Turn ‘ON’ energy loss for IGBT (mJ)
E_{off}	Turn ‘OFF’ energy loss for IGBT (mJ)
f_1	Fundamental inverter frequency (Hz)
f_{clk}	DSP system clock frequency (Hz)
f_{ENCd}	Frequency of encoder pulses A/B (Hz)
f_{swt}	Inverter switching frequency (Hz)
I_{max}	Per phase maximum current that can be supplied by an inverter (A)
i_{sd}, i_{sq}	d - q axis stator currents (A)
i_{sd}^*, i_{sq}^*	Reference d - q axis stator currents (A)
i_s	Instantaneous stator current (A)
J	Motor inertia ($\text{kg}\cdot\text{m}^2$)
K_e	Back EMF/Voltage constant of PMSM (Volt/krpm)
K_T	Torque constant of PMSM (Nm/A)
L_s	Stator per phase inductance (H)
N_{QEP}	Speed of a motor obtained from the eQEP module (RPM)
P	Number of poles
R_s	Stator per phase resistance (Ω)
T_e	Electromagnetic torque (Nm)
T_e^*	Reference electromagnetic torque (Nm)
T_L	External load torque (Nm)
T_0	Dwell time of a zero vector in SVPWM
T_1, T_2	Dwell time of active vectors in SVPWM
v_{ao}, v_{bo}, v_{co}	Inverter terminal voltages/Pole voltages (V)
v_{aN}, v_{bN}, v_{cN}	Inverter phase voltages (V)
v_{ab}, v_{bc}, v_{ca}	Inverter line voltages (V)

v_a, v_b, v_c	Instantaneous three-phase sinusoidal voltages (V)
V_c	Peak to Peak amplitude of carrier wave in SPWM
V_{cc}	IGBT collector voltage (V)
v_{FFQ}	q -axis feedforward compensating voltage (V)
v_{FFQ}	d -axis feedforward compensating voltage (V)
v_{ph}	Load phase voltage (V)
V_m	Peak amplitude of the sinusoidal reference in SPWM
V_{max}	Per phase maximum voltage that can be supplied by an inverter (V)
V_{OFF}	Voltage across IGBT in the ‘OFF’ state (V)
v_{sd}, v_{sq}	d - q axis stator voltages (V)
ω_b	Base speed (rad/sec)
ω_e	Rotor speed (electrical rad/sec)
ω_m	Mechanical rotor speed (rad/sec)
θ_e	Rotor position w.r.t the stator phase ‘ a ’ (electrical rad)
δ	Torque angle (rad)
λ_{airgap}	PMSM airgap flux (Webers)
λ_m	Flux linkage of the permanent magnet mounted on the rotor shaft (Volt • sec)
φ_f	Field flux (Webers)